A Rocky Mountain Storm. Part I: The Blizzard—Kinematic Evolution and the Potential for High-Resolution Numerical Forecasting of Snowfall

GREGORY S. POULOS

Colorado Research Associates, Boulder, Colorado

DOUGLAS A. WESLEY

University Corporation for Atmospheric Research, Cooperative Program for Operational Meteorology, Education, and Training, Boulder, Colorado

JOHN S. SNOOK

Colorado Research Associates, Boulder, Colorado

MICHAEL P. MEYERS

National Weather Service, Grand Junction, Colorado

(Manuscript received 21 June 2001, in final form 22 May 2002)

ABSTRACT

Over the 3-day period of 24–26 October 1997, a powerful winter storm was the cause of two exceptional weather phenomena: 1) blizzard conditions from Wyoming to southern New Mexico along the Front Range of the Rocky Mountains and 2) hurricane-force winds at the surface near Steamboat Springs, Colorado, with the destruction of about 5300 ha of old-growth forest. This rare event was caused by a deep, cutoff low pressure system that provided unusually strong, deep easterly flow over the Front Range for an extended period. The event was characterized by highly variable snowfall and some very large snowfall totals; over a horizontal distance of 15 km, in some cases, snowfall varied by as much as 1.0 m, with maximum total snowfall depths near 1.5 m. Because this variability was caused, in part, by terrain effects, this work investigates the capability of a mesoscale model constructed in terrain-following coordinates (the Regional Atmospheric Modeling System: RAMS) to forecast small-scale (meso γ), orographically forced spatial variability of the snowfall. There are few investigations of model-forecast liquid precipitation versus observations at meso-γ-scale horizontal grid spacing. Using a limited observational dataset, mean absolute percent errors of precipitation (liquid equivalent) of 41% and 9% were obtained at horizontal grid spacings of 5.00 and 1.67 km, respectively. A detailed, high-temporal-resolution (30-min intervals) comparison of modeled versus actual snowfall rates at a fully instrumented snow measurement testing site shows significant model skill. A companion paper, Part II, will use the same RAMS simulations to describe the observations and modeling of the simultaneous mountain-windstorm-induced forest blowdown event.

1. Introduction

During 24–26 October 1997, a deep cutoff low pressure system moved eastward across the southern Colorado Rocky Mountains producing blizzard conditions along the Front Range from Wyoming to southern New Mexico. In addition, this storm caused easterly hurricane-force winds at the surface near Steamboat Springs, Colorado, which destroyed about 5300 ha (1 ha = ~2.5 acres) of west-slope forest. Heavy snow also occurred in Nebraska and Kansas. The effects on the public of these phenomena were immediate and costly: widespread power outages, a crippled international airport, and other transportation-related problems (such as the closure of Interstate Highway 25 (I-25) from the northern to southern border of Colorado simultaneously), hunters stranded in the forest, and thousands of cattle killed. The widespread snow cover associated with this powerful early season storm is characterized well in the visible satellite image shown in Fig. 1a. Because of its occurrence early in the cold season, there was no snow cover on the ground prior to the event, except in the highest elevations of the Rockies. Thus, most of the white areas in Fig. 1a are regions of fresh snow asso-

Corresponding author address: Gregory S. Poulos, Colorado Research Associates, 3380 Mitchell Ln., Boulder, CO 80301.
E-mail: gsp@co-ra.com.

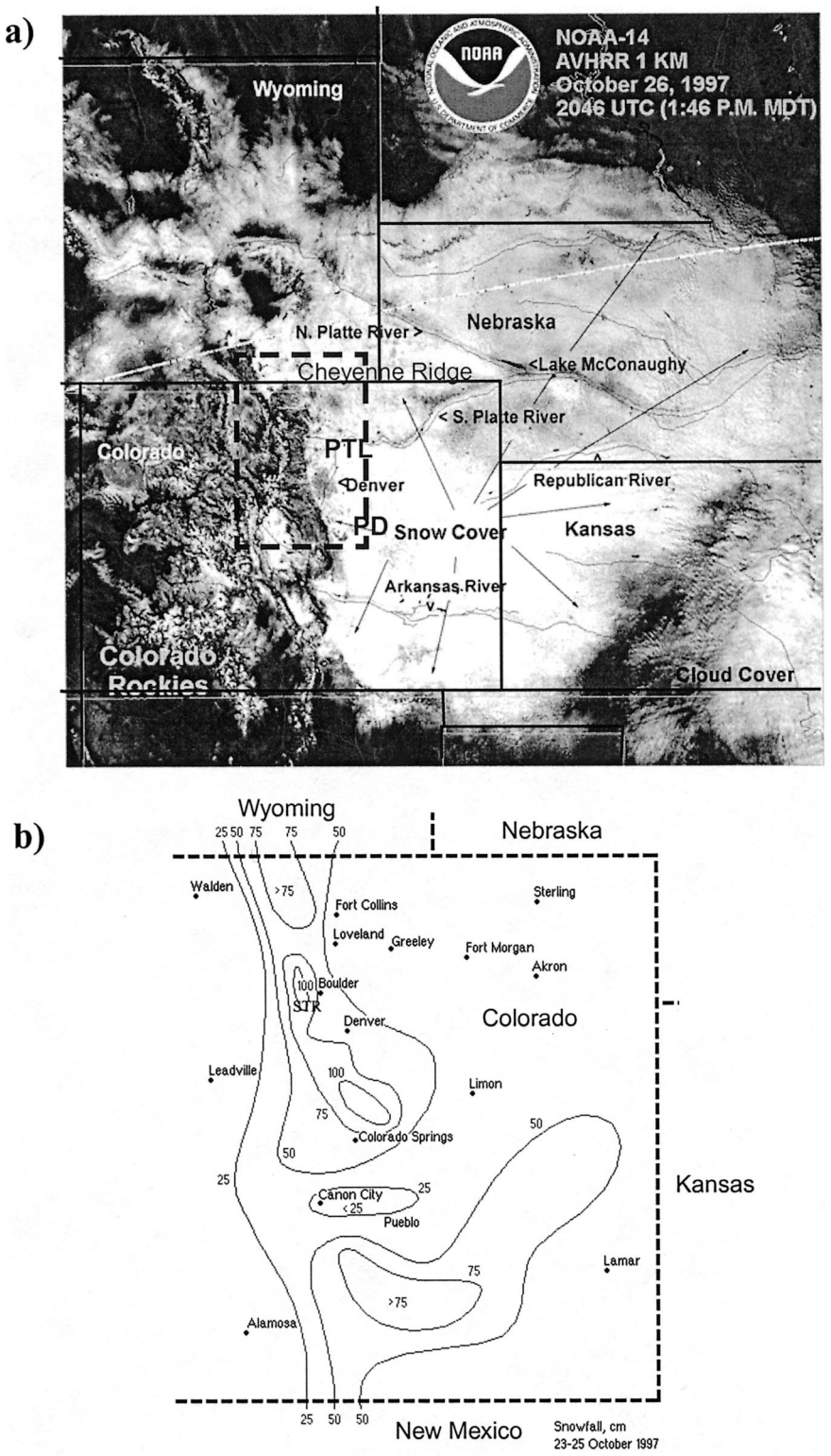

FIG. 1. (a) National Oceanic and Atmospheric Administration (NOAA) Advanced Very High Resolution Radiometer scan of the fresh snowfall coverage from the 24–25 Oct 1997 blizzard: PTL, Platteville wind profiler; PD, Palmer Divide. (b) Snowfall contours from the blizzard for Colorado Front Range. STR is Starr Peak (see also Fig. 9a), where unofficial snow amounts in excess of 1.5 m were reported.

ciated with this system. We focus here primarily on the snowfall in the northern portion of the Colorado Front Range.

This ''upslope'' snowfall event, as is typical for Front Range blizzards (e.g., Wesley et al. 1990; Marwitz and Toth 1993), was characterized by large meso-γ-scale snowfall variability, as well as some very large snowfall totals. Major snow accumulations in Colorado (Fig. 1b) occurred between the morning of 24 October and the evening of 25 October 1997. On spatial scales of approximately 10 km, in some areas, snowfall varied by approximately 1 m. This variability was most pronounced at the mountain–plains interface and across the Continental Divide and could be partially attributed to the fact that rain fell initially on the eastern plains. Prevailing wind speed magnitudes also exhibited strong variability, with threefold differences in speeds observed over the plains on the meso-γ-scale (not shown). Because this variability clearly creates significant problems for operational forecasters, we hypothesized that a mesoscale model with sufficient resolution, initial conditions, and physics—to be specific, adequate cloud microphysics—would be able to forecast snowfall totals, spatial distribution, and storm evolution accurately for this extreme case despite the complication of very complex terrain (e.g. Figs. 1, 8a, and 9a). Furthermore, this case study would serve as a test of the capability of mesoscale numerical weather prediction models in an era of burgeoning applications for them (e.g., Mass et al. 2002). This work compares the output from a high-resolution mesoscale modeling case study with a limited number of standard National Weather Service observations, observations by local meteorological professionals, and observations from a field experiment in Marshall, Colorado.

The mesoscale predictability of precipitation has been discussed in both case studies and longer-term statistical analyses using smaller and smaller grid spacing as computing power has increased. Gaudet and Cotton (1998) report on a comparison of two microphysics methods within the Regional Atmospheric Modeling System (RAMS; Pielke et al. 1992) using grid spacing as small as 16 km over the Colorado Rockies. They find that a bulk microphysical scheme is more accurate than a so-called dump-bucket scheme, with better Heidke skill scores at all precipitation thresholds. Colle et al. (1999, 2000, 2001), Colle and Mass (2000), and Mass et al. (2002) report on multiyear statistics of numerical weather prediction for the northwestern United States. Those studies are representative of precipitation forecasts for horizontal grid spacings of 4, 12, and 36 km, using the fifth-generation Pennsylvania State University–National Center for Atmospheric Research Mesoscale Model (MM5; Dudhia 1993) and the National Weather Service Eta Model using 10-km horizontal grid spacing (Eta-10). Colle et al. (1999) find that MM5 forecasts have greater precipitation forecast skill over the northwestern United States using 12-km grid spacing versus 36-km grid spacing, although precipitation is overestimated (underestimated) on windward (lee) slopes. Furthermore, it was found that the Eta-10 was less accurate overall, when compared with MM5 using 12-km grid spacing, although at low precipitation thresholds the Eta-10 had lower root-mean-square error.

Extending this work, Colle et al. (2000) present extensive statistical analysis of precipitation forecast accuracy over the Pacific Northwest. In this work, Colle et al. find that for smaller precipitation thresholds (defined as <5.08 cm day^{-1}), decreasing horizontal grid spacing from 36 to 12 km noticeably improves bias, equitable threat, and root-mean-square error scores. However, in contrast to our hypothesis, decreasing horizontal grid spacing further to 4 km, for smaller precipitation thresholds, worsens these same skill scores. However, at higher precipitation thresholds (e.g., >5.08 cm day^{-1}), decreasing horizontal grid spacing from 12 to 4 km improved skill scores. If these results were to be generally applicable beyond the Pacific Northwest of the United States, to other mesoscale models and were extrapolated to this case study in which the maximum precipitation rate was 4.0 cm day^{-1}, it would suggest that no improvement in skill would be found by decreasing horizontal grid spacing from 5.0 to 1.67 km.

2. Storm kinematics

Overall, this event was strongly forced on the synoptic scale, with significant terrain-forced factors superimposed, such that the heaviest snowfall occurred in the foothills of the Front Range and the western portion of the Palmer Divide (Fig. 1b). Strong winds caused blizzard conditions over Colorado's eastern plains and snowdrifts up to 5 m (P. Wolyn 1997, personal communication). Heavy snowfall was not confined to Colorado's eastern foothills; the southeastern Wyoming mountains received up to 0.75 m of snow on 23–24 October (D. Moore 1997, personal communication), and heavy snow also occurred on 25 October over southeastern Colorado.

A deep, cutoff low pressure system was located over the Four Corners region during the day on 24 October (Fig. 2) in partial response to an intensifying jet maximum over the desert Southwest (not shown). Heavy snowfall and blizzard conditions first developed over southeastern Wyoming late in the afternoon of 24 October after a cold front moved south ahead of the strengthening upslope flow. Although the center of the surface low pressure system was over the Texas Panhandle, the mean sea level pressure gradient over northeast Colorado was oriented N–S and was strong late in the day. Also, a strong NW–SE-oriented 700- and 850-hPa height gradient existed over northeast Colorado by 1800 UTC 24 October.

The combination of strong upslope low-level flow, ample moisture, and significant large-scale ascent in response to the deepening cutoff low pressure system pro-

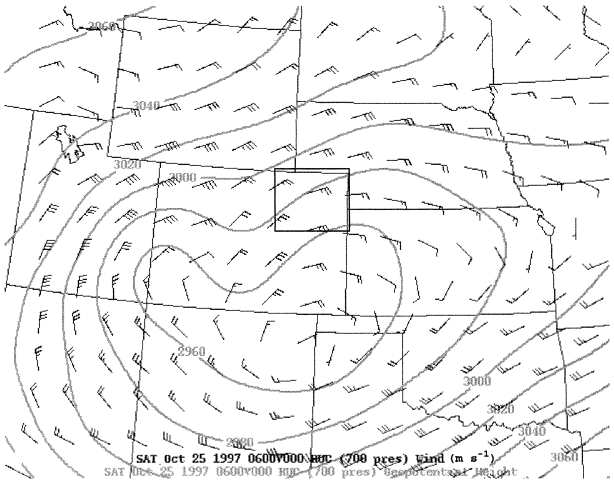

FIG. 2. The 700-hPa height (m MSL, contour interval 20 m) RUC analysis from NOAA for 0000 UTC 25 Oct 1997 and wind barbs, showing the cutoff low pressure system over southern Colorado. Full and half barbs represent winds of 5.0 and 2.5 m s^{-1}, respectively. A rectangle shows our study area.

duced deep clouds (Fig. 3) and heavy precipitation over north-central and eastern Colorado, southeastern Wyoming, and the Nebraska Panhandle by 0000 UTC 25 October. By 0300 UTC 25 October, winds from the east-northeast of 10–15 m s^{-1} were present at the surface over northeastern Colorado and southeastern Wyoming. Detailed examination of radar features using the Denver, Colorado, (DEN) and Cheyenne, Wyoming, (CYS) Next-Generation Weather Radar data revealed no significant banded structure in the precipitation although loops of these radar scans clearly indicated enhanced reflectivity regions associated with foothills orography to the west and south of the urban corridor (not shown). Also noteworthy were the shortcomings of the radar data in capturing some intense snowfall regions in these foothills, in part because of clutter removal and beam overshooting.

Profiler data at Platteville (Fig. 4), located in Colorado about 50 km north of Denver (see Fig. 1), added critical operational information about the temporal evolution of the storm kinematics. As the intense cutoff low pressure developed to the southwest of this location, the predominantly easterly winds in the 3–6 km MSL layer (1.5–4.5 km AGL) strengthened significantly to 15 m s^{-1} by 0600 UTC 25 October and to 20 m s^{-1} 6 h later. This enhancement was correlated with the intensifying precipitation over the northern Colorado Front Range. Low-level ageostrophic northerly winds were primarily confined to the lowest 500 m AGL and were the result of the deepening surface low pressure over southeastern Colorado and the Texas Panhandle. Part II of this study (Meyers et al. 2002, manuscript submitted to *Wea. Forecasting*) discusses the role of the strong easterly winds aloft, and associated moist mountain wave dynamics, in creating conditions conducive to a simultaneous powerful windstorm on Colorado's western slope.

Like for many other Front Range blizzards (e.g., Wesley et al. 1990; Marwitz and Toth 1993; Szoke 1989), large horizontal gradients in both total snowfall and snowfall rates characterized the precipitation (Fig. 1b).

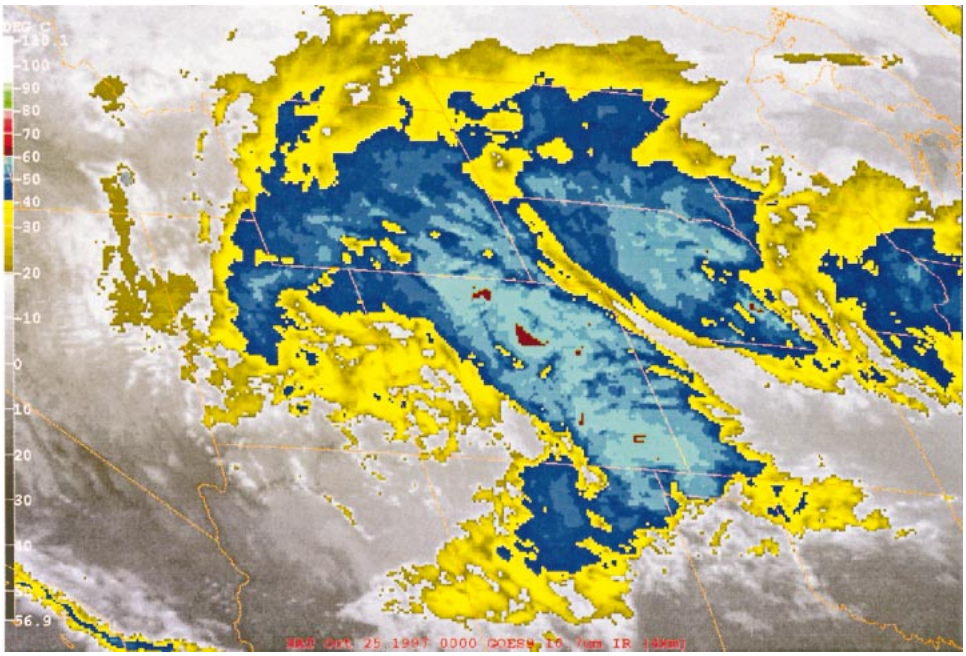

FIG. 3. NOAA *Geostationary Operational Environmental Satellite-8* local IR cloudiness over the Colorado region for 0000 UTC 25 Oct 1997.

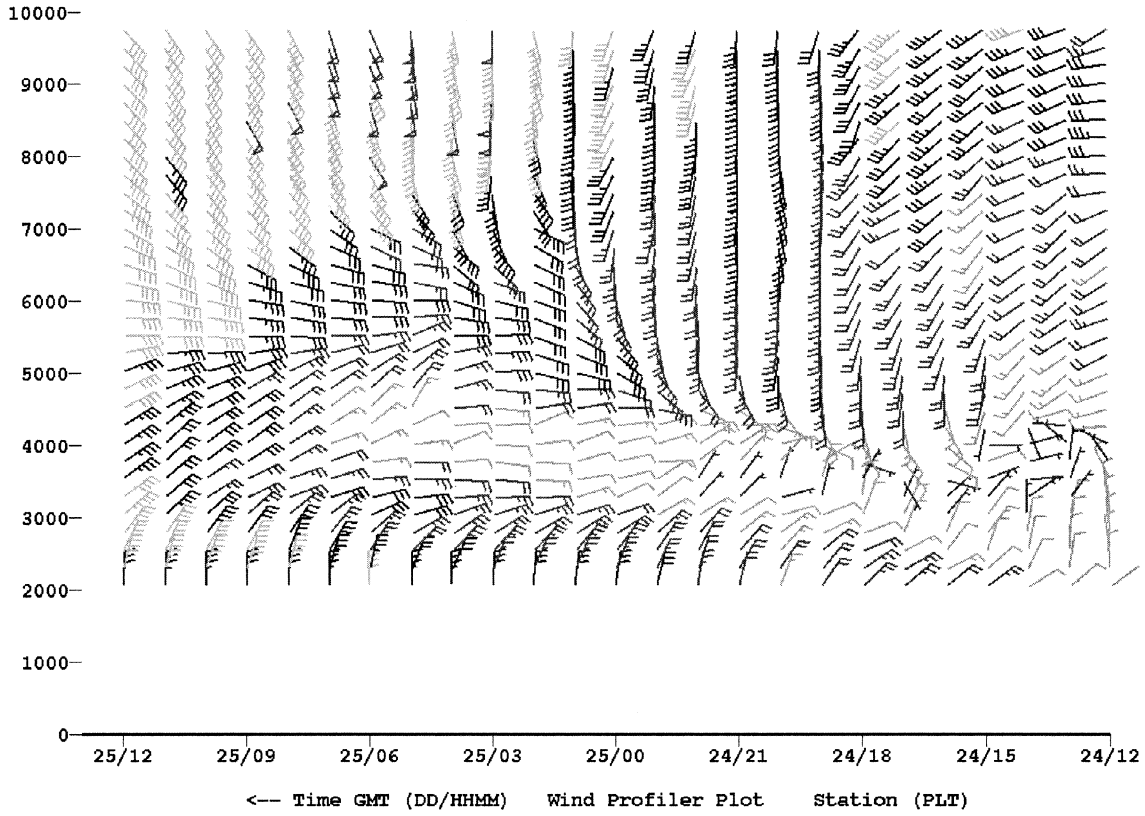

FIG. 4. PTL wind profiler wind barbs to 10 000 m MSL showing deep, strong easterly flow responsible for prolonged upslope snowfall over the Front Range. PTL is located near I-25 about 50 km north of Denver, CO (Figs. 1 and 8a). Full and half barbs represent winds of 5.0 and 2.5 m s^{-1}, respectively.

For example, the portion of the urban corridor near I-25 north of Denver generally received 0.25–0.5 m of total snowfall while totals of 0.65–0.9 m were common in areas 10–20 km west of I-25, with extremes exceeding 1.5 m in favored foothill locations [see STR (Starr Peak) in Fig. 1b; note that a 1.5-m contour is not drawn]. Large variation also characterized the snow density in this storm, which began as rain on the Colorado plains. Snow-to-liquid ratios ranged from 10:1 (wet snow) to 25:1 at some higher-elevation locations (in general, lower snow density characterized the latter period of the storm in all areas).

Another important aspect of the snowstorm was the large variability in wind speeds observed within the heavy snow regions on the plains and foothills. Some areas (near and around Boulder, Colorado, for example; Fig. 1b) experienced only 5–10 m s^{-1} wind speeds during heavy snowfall; others (e.g., the Denver International Airport region) were crippled by 15–25 m s^{-1} gusts (not shown) that generated large snowdrifts and near-zero visibility, wreaking havoc on airport and forecast operations and the rural populace.

Deceleration within a blocked flow regime to the lee (south) of the Cheyenne Ridge (Wesley et al. 1995) west of I-25 may have played a significant role in this wind distribution. The so-called Longmont anticyclone is a region of low-level convergence and enhanced lift typically located between the Fort Collins–Longmont area (see Fig. 1b) and the western suburbs of Denver during large-scale northerly flow regimes. It is a result of terrain-induced blocking processes associated with the Cheyenne Ridge and Palmer Divide (see Fig. 1a). The Longmont anticyclone is often responsible for decreased wind speeds and snowfall enhancement in this region. In the 24–25 October 1997 event, synoptic forcing was very strong, but reduced wind speeds typical of the Longmont anticyclone, measured in Boulder and nearby stations, correlated with extremely high snowfall rates caused, in part, by low-level convergence.

The storm evolution in southeastern Colorado, which also experienced heavy snowfall, was similar to but delayed relative to that of the northern Colorado Front Range. Rain initially was widespread over the southeastern plains. After the cold front moved southward late on 24 October, the large-scale uplift continued to intensify, and precipitation quickly changed to snow. The synoptic forcing was well illustrated with strong isentropic uplift over the southeastern plains on 25 October. Continued cyclogenesis over southwest Kansas produced snowfall until early on 26 October in southeastern Colorado.

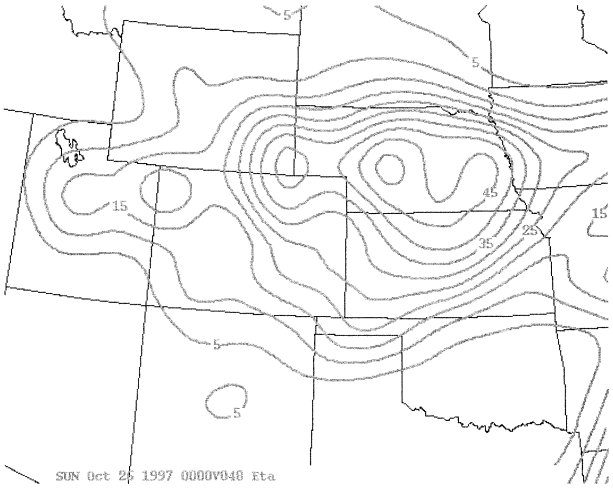

FIG. 5. The NCEP Eta Model's forecast of 48-h accumulated precipitation (mm) valid at 0000 UTC 26 Oct 1997.

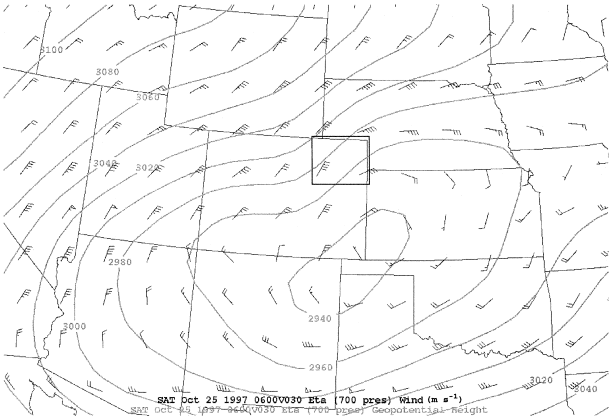

FIG. 6. The Eta 30-h prediction of 700-hPa winds and geopotential height (m MSL, contours are in 20-m intervals) for 0600 25 Oct 1997. Full and half barbs represent winds of 5.0 and 2.5 m s^{-1}, respectively.

3. NCEP model guidance

Capturing the details of a precipitation/wind event manifested on the meso-γ (2–20 km) scale within a model requires the highest grid resolution possible given the restriction of providing useful forecasts in real time. Resolution improvements in National Centers for Environmental Prediction (NCEP) models are providing advances in the usefulness of regional/mesoscale models in forecasting winter storm events in the Rocky Mountains (Rogers et al. 2001; Junker et al. 1989). Numerical guidance for the 24–25 October 1997 storm was particularly accurate and useful given the relatively coarse grid spacing still present in the Rapid Update Cycle (RUC), Eta Model, Aviation Model, and Nested Grid Model at that time (as of May of 2001 these grid spacings were 40, 32, 60, and 48 km, respectively).

Eta forecasts (e.g., Fig. 5) indicated the likelihood of heavy snowfall well in advance (48 h), but only 15–30 mm of liquid precipitation was forecast for Colorado's east-central foothills, where 35–60 mm fell in general. In the northern foothills, model precipitation estimates were somewhat higher (~35 mm near the Wyoming border). Forecasters with access to this and earlier Eta forecasts could have predicted a heavy snowfall event in the Colorado Front Range and plains (and did so based on their knowledge of local terrain and weather) but likely could not have elucidated much further on snowfall distribution and the potential for an extreme event, based on this numerical guidance.

The potential for strong low-level winds west of the Continental Divide was present in Eta and Meso-Eta forecasts. However, some subtle errors in the wind predictions could have led to serious errors in forecast precipitation east of the divide. For example, the Eta prediction at 30 h of 700-hPa heights (~3 km MSL) and winds (Fig. 6) contained north-northeasterly winds of about 20 m s^{-1} over the northern Front Range of Colorado. The actual winds at 0600 UTC 25 October, as discussed previously and in Fig. 4, were from the east-northeast at about 15 m s^{-1}, at 3 km MSL. This condition is much more favorable for strong upslope forcing and precipitation. Though the general features in the forecast verified well qualitatively, even relatively subtle errors in wind direction have the potential to make the difference between light snow and heavy snow in this region (Szoke 1989). Another example of an important error in model precipitation forecasts, from the 1200 UTC 24 October Eta forecast (~6 h after the start of precipitation on the Front Range), is shown in 12-h accumulated precipitation valid at 0600 UTC 25 October (Fig. 7). Though the 850-hPa height analysis implied strong geostrophic upslope conditions over northeastern Colorado and the foothills, the 12-h precipitation amounts in that region were underforecast by nearly twofold, particularly over the foothills to the west.

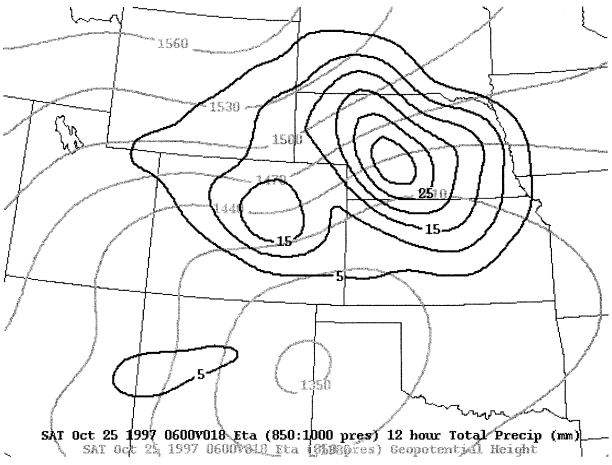

FIG. 7. The Eta Model 12-h (1800–0600 UTC) accumulated total precipitation (mm) and 850-hPa geopotential height (m MSL, contours are in 30-m intervals) valid at 0600 UTC 25 Oct 1997 from the 1200 24 Oct 1997 model run.

It is evident that much finer detail in model results could be used (given an accurate large-scale forecast) by forecasters to apply model data for improved predictions of wind and snowfall distributions in storms similar to that of 24–25 October 1997. Large gradients in wind magnitude and snowfall occurred on scales far below even the Meso-Eta grid spacing. The nested mesoscale model simulations produced by local models such as RAMS (Pielke et al. 1992), the Coupled Ocean–Atmosphere Mesoscale Prediction System (Hodur 1997), and MM5 (Dudhia 1993) have potential for addressing this problem, as described below.

4. Modeling description

The model used was RAMS version 3a, a prognostic, nonhydrostatic, primitive equation, mesoscale model developed at Colorado State University (Pielke et al. 1992). Advective and source terms are time differenced using a basic leapfrog formulation and Asselin filter, turbulent quantities are time differenced using a forward scheme, and acoustic terms are time differenced using a forward–backward semi-implicit scheme over a smaller time step than is used for the other terms (because of the high speed of sound waves relative to typical atmospheric motions). Of particular interest to the forecasting problem of the Front Range of the Rockies is the use of terrain-following coordinates combined with horizontal grid nesting. This nesting allows the grid spacing to be reduced over a specific geographic area of interest.

Two different microphysical schemes were used in this study. First, RAMS includes a mixed-phase microphysical scheme described by Walko et al. (1995). The model prognostic fields are the mixing ratios of raindrops, pristine ice crystals, snow, aggregates, graupel, and hail, respectively, from which the cloud droplet mixing ratio is diagnosed. Each of these water categories is distributed according to a generalized gamma distribution. Schultz (1995) describes a microphysical scheme, which is simpler, using fewer hydrometeor categories and microphysical interactions, and which is more computationally efficient than the RAMS microphysics described briefly above. A thorough description of the various features of RAMS can be found in Pielke et al. (1992) and is not included here.

To utilize RAMS in a forecasting mode, analyses of the NCEP Eta at $\Delta x = \Delta y = 48$ km (north–south and east–west horizontal directions, respectively) were used for initialization, and Eta forecasts of atmospheric conditions in 12-h intervals were used for subsequent nudging at the outer model boundaries (at the time of this event, the NCEP Eta was initialized at 0000 and 1200 UTC and was integrated for 48 h). Three simulations were completed. The first simulation, hereinafter labeled Bliz60S1, was configured so as to encompass the entire period of snowfall, the 60-h period from 0000 UTC 24 to 1200 UTC 26 October. Once initialized using the Eta analysis at 0000 UTC 24 October 1997, the model solution was then nudged toward, first, the 1200 UTC 24 October Eta analyses and, thereafter, the appropriate four consecutive Eta forecasts at 12-h intervals. This procedure could be executed for real-time forecasting today, with the longer Eta runs from the National Weather Service (NWS) now available, but, in this case, two consecutive Eta analyses were used to nudge the first two fields and then the forecasts from Eta were used thereafter. The cloud microphysics scheme given by Schultz (1995) was used in Bliz60S1 because it is more computationally efficient and may be more effective in a day-to-day forecasting operation. Thus, although simulations are faster, they risk missing some less frequently seen, but possibly important, precipitation mechanisms. For comparison, a second simulation, labeled Bliz60R1, using the RAMS full microphysical package (Walko et al. 1995) was completed. It was otherwise exactly the same as Bliz60S1 above. A third simulation using Schultz (1995) microphysics was also completed that was 48 h in duration beginning at 1200 UTC 24 October. It began 12 h later than Bliz60S1, with slightly smaller inner nests, with the purpose of mimicking a real-time forecasting configuration given that the Eta Model runs were only 48 h in length in 1997. We refer to this simulation as Bliz48S2 in the upcoming discussion.

To accomplish snowfall prediction on small scales requires some means by which to use high resolution in the region of interest while not sacrificing the larger scales that are crucial to the dynamics of this synoptic event. To do so, multiple nested grids were employed to focus on the region in which snowfall variability and terrain relief were greatest, that is, at the mountain–plains interface. The outermost grid encompasses part of the western and central United States to allow for the synoptic evolution of the storm system over a 60-h simulation period (not shown). The second grid (or the first nest) telescopes in on the Front Range of northern Colorado (see Fig. 8a). The innermost nest (grid 3; see Fig. 9a) captures the local region in Colorado in the foothills west of the Denver–Boulder corridor, where the storm snowfall maximum occurred (limited to the accuracy of observations). Starr Peak (STR), a local mountaintop within the foothills that received a local maximum of snowfall (>1.5 m, unofficially), is marked in Figs. 8a and 9a. The Marshall test site (MAR), where a snow gauge testing experiment was coincidentally under way during the blizzard (Wade et al. 1998), is marked in Fig. 9a.

Grid 1 (not shown) had $\Delta x = \Delta y = 15$ km and covered a domain of 900 km $\times$ 900 km $\times$ 18 km with $61 \times 61 \times 50$ grid points. Grid 2 was nested at a 3:1 ratio, resulting in $\Delta x = \Delta y = 5$ km over a 380 km $\times$ 395 km $\times$ 18 km domain with $77 \times 80 \times 50$ grid points (Fig. 8a). The innermost nest also had a 3:1 ratio within grid 2, resulting in $\Delta x = \Delta y = 1.67$ km over a region of 112 km $\times$ 87 km $\times$ 18 km with $68 \times 53 \times 50$ grid

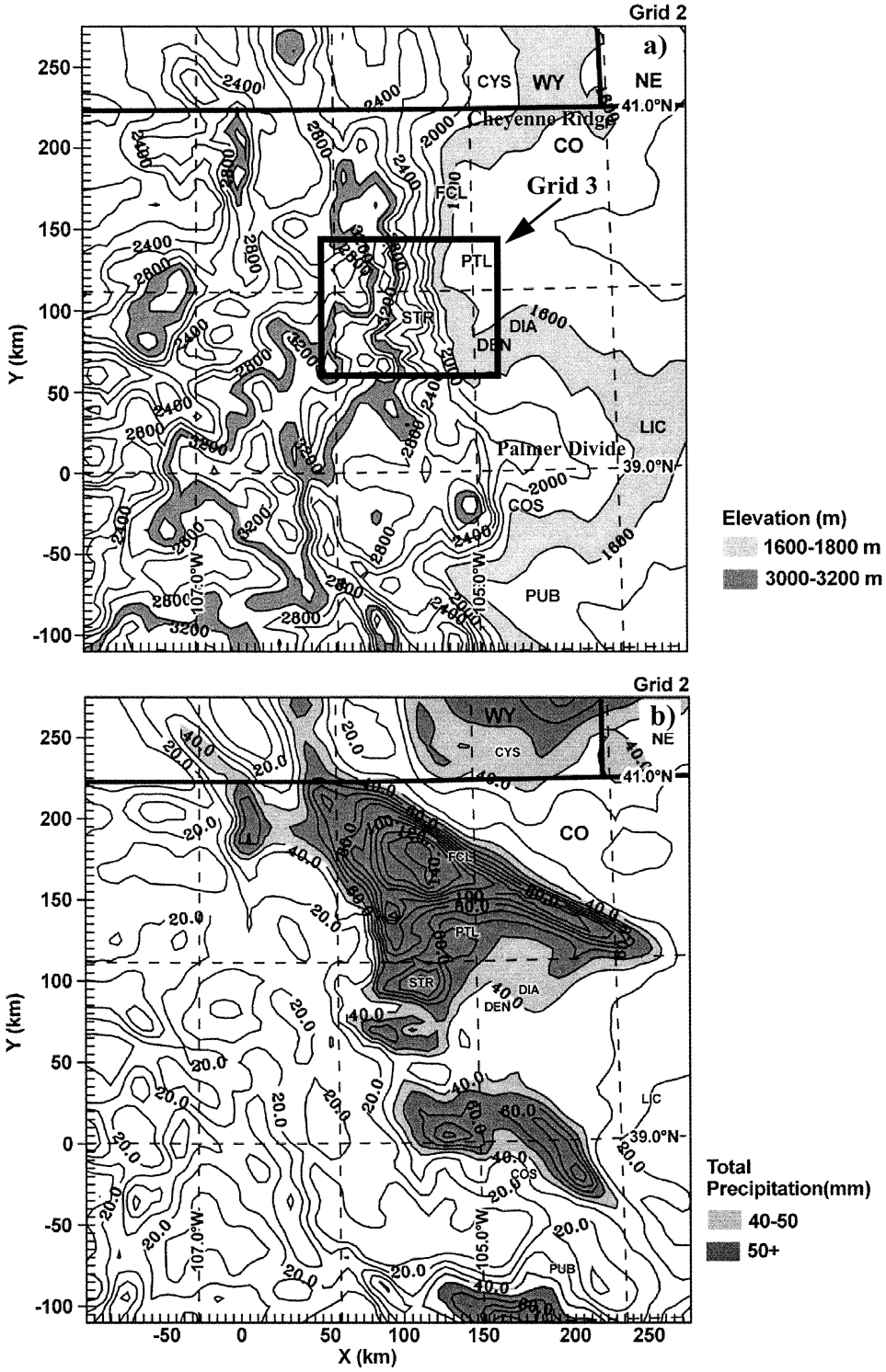

FIG. 8. (a) The topography (200-m contour intervals) of the study area from grid 2 (of three grids) of the RAMS simulation Bliz60S1. The southwest corner of this grid is at 38.01°N, 107.79°W, and lat–lon lines are in 1.0° intervals. The grid-3 domain is indicated for reference (see Fig. 9 for details). (b) Accumulated 60-h total liquid precipitation on grid 2 for run Bliz60S1 (valid 1200 26 Oct 1997). Contours are in 10-mm increments. Symbols: COS = Colorado Springs, CO; CYS = Cheyenne, WY; DEN = Denver, CO; DIA = Denver International Airport, CO; FCL = Fort Collins, CO; LIC = Limon, CO; and PUB = Pueblo, CO.

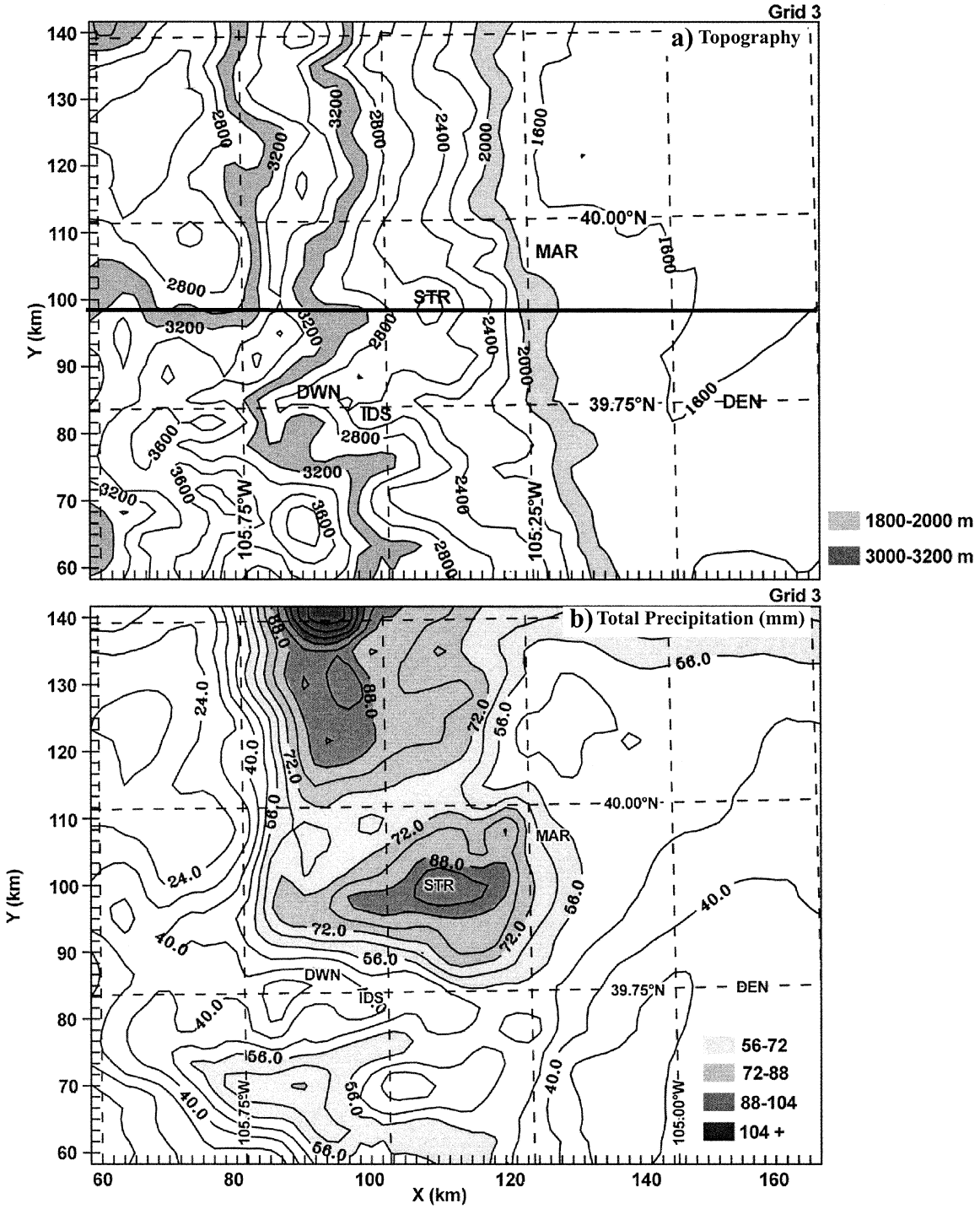

FIG. 9. (a) Topography (200-m contour interval) for grid 3, the innermost nest, for run Bliz60S1. The southwest corner of the domain is 39.52°N, 106.02°W, and 0.25° lat–lon increments are shown. The dashed line indicates the location of the *x–z* cross section in Fig. 10. The oval encircles the area within which local liquid precipitation measurements were available. (b) The 60-h forecast liquid total precipitation on grid 3 ($\Delta x = \Delta y = 1.67$ km) for run Bliz60S1 for the Oct 1997 blizzard in the Front Range of Colorado. Contours are in 8-mm increments, with one maximum of 104 mm at STR. See Fig. 8a for the location of grid 3 within grid 2. Symbols (all in CO): DEN = Denver, DWN = Downieville, IDS = Idaho Springs, BOU = Boulder, and MAR = Marshall test site.

points (Fig. 9a). Typical, no-slip boundary conditions in which horizontal winds are assumed to become zero at the earth's surface were used. These simulations are an example of next-generation numerical weather prediction capabilities that could be run operationally on a day-to-day basis using the currently available computing technology, analyses, and boundary conditions.

5. Results

One of the most important factors in the perception of an accurate forecast is capturing the onset and duration of precipitation. With the relatively lower resolution of current NCEP models and delivery of such models in relatively coarse time intervals (currently 3 h for Eta 3D and 2D meteorological fields, but soundings available to the forecaster in hourly intervals), the ability of operational forecasters to provide this information in complex terrain regions is limited. However, as previous studies (Snook et al. 1995) and these simulations show, the timing of a snowstorm at a specific location can be captured very accurately with better resolution and more frequent delivery of model fields. In general snowfall began in earnest in the northern two-thirds of Colorado during the period 1200 UTC 24–0000 UTC 25 October, continued heavily for the next 12 h (overnight Friday), and tapered off during the day on 25 October. This evolution and in particular the heavy snowfall overnight Friday were captured by the RAMS forecast. The scope of the majority of the following discussion pertains to all three runs—Bliz60S1, Bliz48S2, and Bliz60R1—even though the focus is on Bliz60S1 (which had the most accurate precipitation evolution).

Figure 10 shows that strong easterly, barrier-perpendicular, flow (generally 15–20 m s^{-1}) up to 6 km above the lowest model topography combined with uplift of more than 0.2 m s^{-1} in the eastern foothills (Fig. 10b) created significant upslope snowstorm conditions. This cross section is east–west on grid 3 through the location of the southern snowfall maximum from Bliz60S1 (as indicated by the dashed line in Fig. 9a) at 0600 UTC 25 October (Friday evening) during some of the most consistent, heavy snowfall. Potential temperature isopleths indicate a layer of more stable air from about 2000 to 3200 m that slopes gently upward to the west. This layer contains the maximum u-component (east–west) winds. The lifting estimated from this orientation of potential temperature lines relative to the observed vertical velocity w in Fig. 10b is low because of the well-known influence of moisture on potential temperature [e.g., see θ_{i1}, θ_{ie}; Cotton and Anthes (1989, chapter 2)] and diabatic processes. Note also the strong accelerated easterly downslope flow in the lee (west) of the Continental Divide at x approximately equal to 80 km, which is an indication of the potential for a west-slope windstorm (see Part II). The pattern of r_{ice} shows that maximum values of snowfall at this time fell on Starr Peak, which corresponds well to the observed local maximum in snowfall of over 1.5 m along the northern Front Range in this area (this isolated observation is not portrayed with a contour in Fig. 1b because of contour smoothing). To the west of $x = 90$ km, r_{ice} steadily decreases, corresponding to drying in the lee, as was also illustrated in Fig. 1b.

All of the simulations were successful in reproducing patterns of meso-γ-scale variability of snowfall during the blizzard, and Bliz60S1 was particularly accurate in total precipitation. Figure 8b shows the Bliz60S1 forecast total liquid precipitation after the full 60 h of simulated time. An obvious general correspondence between elevation, particularly on northeast-facing slopes, and snowfall exists on the east side of the Continental Divide (roughly enclosed by the 3000–3200-m gray shading in Fig. 8a), with a vast reduction in snowfall in the lee (west) side, as was observed during the storm.[1] The relative maxima on the plains on the north side of the Palmer Divide correspond to the observed maximum as shown in Fig. 1b. It is unclear, because of the lack of snow observations on the northeastern plains of Colorado, whether the NW–SE-oriented snowfall maximum in Fig. 8b is realistic. This potentially spurious maximum provides an example of the difficulty in using high-resolution forecast information by a forecaster. Given a ≥48-h forecast of such a maximum, a forecaster would have to decide whether it was to be believed, whereas a lower-resolution forecast, such as in Fig. 5, does not present the same issue. Overall, when combined with a forecaster's experience, we speculate that the grid-2 total precipitation field would aid the forecaster in discriminating snowfall variability. The accuracy of grid-2 total precipitation is verified quantitatively below.

In contrast to the results of Colle et al. (2000), grid 2 was less accurate than the higher-resolution grid 3. Figure 9 shows plots of relatively higher resolution grid-3 ($\Delta x = \Delta y = 1.67$ km) topography (Fig. 9a) and the 60-h total precipitation on grid 3 (Fig. 9b) from Bliz60S1. As also shown in Fig. 8b for grid 2, terrain has a distinct influence on precipitation patterns and reveals the importance of three-dimensional orographic effects on precipitation patterns, which are superimposed on the larger-scale synoptic forcing of precipitation. As expected, the further refinement of grid spacing on this grid has resulted in a reduction in the scales of precipitation variability as was found by Snook et al. (1995). For example, over an approximately 20 km distance on a line starting from STR to Downieville (DWN) precipitation varies by more than 60 mm. Using an average snow depth–to–liquid depth ratio of 12:1 from the storm, this results in a snowfall differential of more than 0.75 m. Snowfall differences of this magnitude and larg-

[1] Amusingly, Colorado ski areas experienced a major increase in reservations after the national news coverage of the blizzard, although, with the exception of east-slope ski areas, very little snow was received there.

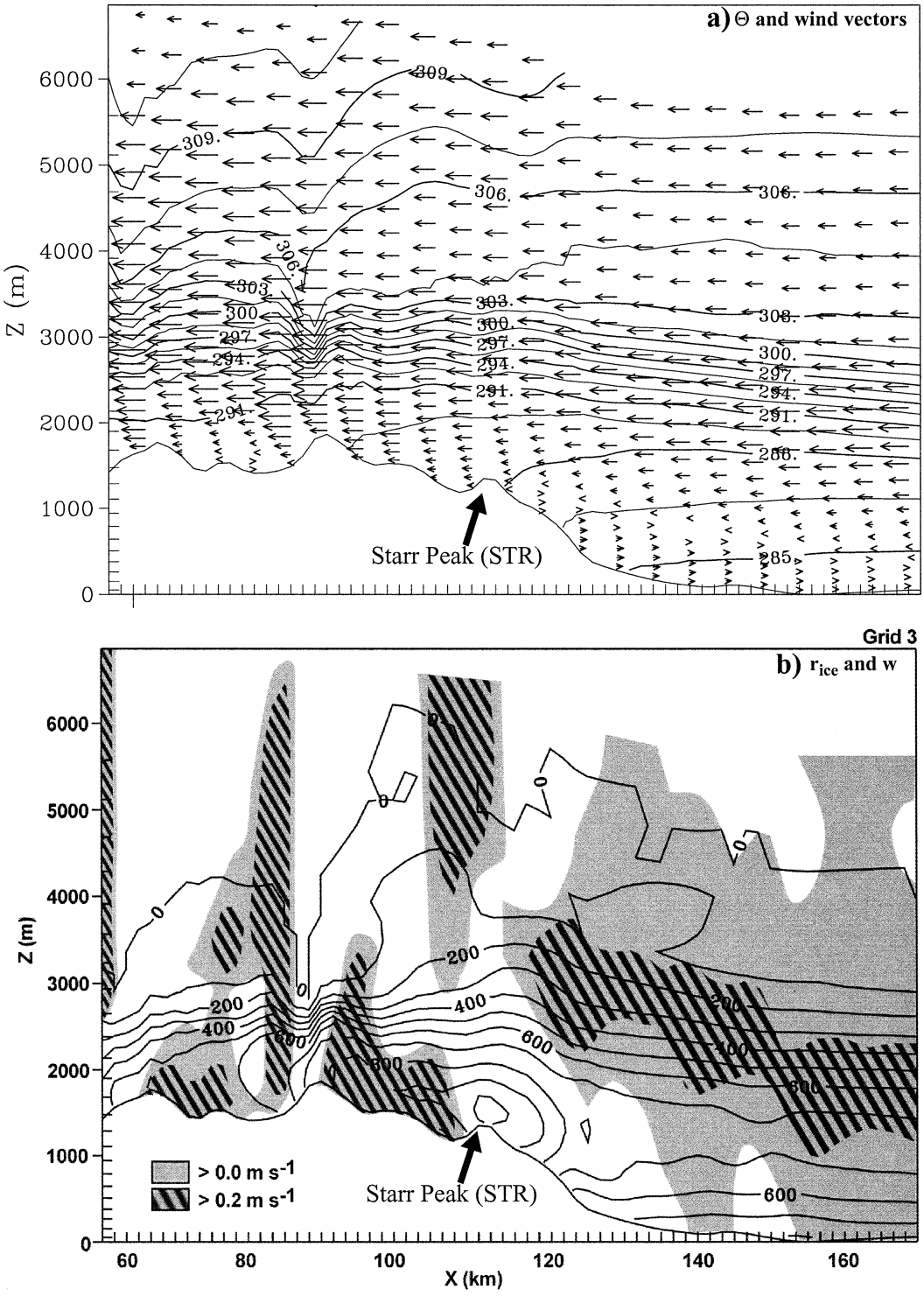

FIG. 10. An east–west (x–z) cross section on grid 3 for run Bliz60S1 at 0600 25 Oct 1997 of (a) potential temperature (1.5-K increments) and u wind vectors (maximum vector of 28 m s^{-1}) and (b) r_{ice} (total ice mixing ratio; contours: g kg^{-1} × 10^3) through STR on grid 3 (see dashed line in Fig. 9a for location). Regions of positive w are shaded at >0.0 and >0.2 m s^{-1}. This was a period of intense but realistic precipitation rate as compared with ETI-Wyoming gauge precipitation rate observations (see Fig. 11) from MAR. Note the maximum of ice mixing ratio at STR.

TABLE 1. Precipitation observations for the Oct 1997 Rocky Mountain Front Range blizzard vs forecast precipitation from two 60-h RAMS simulations: Bliz60S1 and Bliz60R1. Grid-3 sites are those precipitation observational sites exclusively located within grid 3. Grid-2 sites are those precipitation observational sites exclusively located in grid 2. MAPE = mean absolute percent error; see Eqs. (1) and (2) for definitions.

Location	Observed snowfall (liquid mm)	Bliz60S1 forecast precipitation % error	Bliz60R1 forecast precipitation % error
Grid-3 ($\Delta x = \Delta y = 1.67$ km) sites			
1. Coal Creek Canyon, R. Keen	76	+5.2	+2.6
2. Residence, K. Wolter	69	+11.6	+5.8
3. Marshall test site	59	+4.3	−22.0
4. Boulder cooperative station	57	+22.8	−19.3
5. Residence, M. Kelsh	57	+3.5	−15.8
6. Residence, P. Neiman	57	+19.2	+10.5
7. Residence, P. Stamus	55	−9.1	−10.9
8. Residence, E. Szoke	51	+2.0	−5.9
9. Residence, T. Schlatter	48	+2.0	−2.0
Grid-2($\Delta x = \Delta y = 5.00$ km) sites			
10. Fort Collins, CO (FCL)	45	+77.7	+22.2
11. Denver International Airport (DIA)	35	+20.0	+71.4
12. Colorado Springs, CO, airport (COS)	24	+8.3	+91.7
13. Cheyenne, WY, airport (CYS)	24	+45.8	+108.3
14. Pueblo, CO, airport (PUB)	18	+33.3	+344.4
Overall MAPE		18.8	52.3
Grid-3 ($\Delta x = \Delta y = 1.67$ km) MAPE		8.9	10.5
Grid-2 ($\Delta x = \Delta y = 5.00$ km) MAPE		41.3	127.6

er were observed after the storm by the authors. Of course, the actual snowfall variability was greater than even grid 3 can resolve, because of poor representation of certain microscale terrain features and the inability to characterize detailed evolution of orographic storm dynamics, blowing, and drifting snow adequately.

The precipitation forecast accuracy of Bliz60S1 and Bliz60R1 is presented in Table 1, which shows the precipitation observation O and the percent error (%error) of the forecast precipitation F relative to grid number (and therefore, grid spacing), where

$$\%\text{error} = \left[\frac{(F - O)}{O}\right] \times 100\%. \quad (1)$$

At the bottom of Table 1, the mean absolute percent error (MAPE) for all data (sample size $N = 14$), grid-3 data only ($N = 9$), and grid-2 data only ($N = 5$) is presented, where

$$\text{MAPE} = \frac{1}{N}\sum_{i=1}^{N}\left|\left[\frac{(F - O)}{O}\right] \times 100\%\right| = \frac{1}{N}\sum_{i=1}^{N}|\%\text{error}|. \quad (2)$$

As is often the case, accurate precipitation observations are more difficult to obtain than are accurate snowfall observations, and, thus, the data available for direct comparison with the model were somewhat limited. On the other hand, if one considers that no organized field project was in progress to make these observations, with the exception of the Marshall site, it is remarkable that there are so many liquid precipitation observations available. The observations shown in Table 1 were provided by NWS official recordings, NWS cooperative sites or professional meteorologists from the region. Additional precipitation data were available from Snowpack Telemetry sites but because of the early cold season occurrence of this storm they were subject to large errors and were therefore inadequate for this comparison. The comparison with observations should be tempered by the fact that precipitation measurements of snowfall, because of wind, topography, and storm evolution, can vary significantly, perhaps by more than 20% (Doesken and Judson 1997; N. J. Doesken, 2000, personal communication). On grid 2 (5-km horizontal grid spacing), the MAPE relative to the observations is 41% with the Schultz (1995) modification and 127% with the full RAMS microphysics (Walko et al. 1995). Although it is clear in this case that the Schultz modification has outperformed the RAMS bulk microphysics, this is statistically insignificant because of the singular comparison, and it is not possible to endorse one over the other.

The inability to evaluate the performance of microphysical schemes is made more difficult by the results on grid 3, on which the performance differential reduces significantly between them. On grid 3, which used horizontal grid spacing of 1.67 km, the results improve, perhaps surprisingly when compared with the implications of Colle et al. (2000) and Mass et al. (2002). The MAPE of precipitation for Bliz60S1 is 9% and the MAPE for Bliz60R1 is 11%. If one considers that normal errors in snowfall measurements, including liquid precipitation, often exceed these percentages (Doesken and Judson 1997), this comparison is excellent. One obvious and plausible cause of the reduction of error

between the 5.00-km horizontal grid spacing on grid 2 and the 1.67-km horizontal grid spacing on grid 3 is the improved representation of orographic influence on precipitation magnitude and distribution. Combined with potentially improved resolution of mesoscale precipitative processes in the storm itself, the result is a reduction in the MAPE.

Another significant factor in the evaluation of the difference between the grid-3 and grid-2 precipitation results is the scale of separation between the observations as compared with the driving scales within the storm system and terrain. To be specific, the distance between observations used for verification on grid 2 [see Table 1 and Fig. 8a; a maximum of ~300 km from Pueblo, Colorado, (PUB), to CYS] is much larger than that on grid 3 (Boulder and vicinity, a maximum of ~35 km; see oval in Fig. 9a). Also, grid 2 is considerably larger than grid 3. Furthermore, the storm system (e.g., Fig. 3) and terrain have significant subsynoptic-scale features. Thus, if the simulated total precipitation in the vicinity of Boulder was predicted well for this individual case as compared with other locations regardless of 5.0- or 1.67-km grid spacing, then the comparison with observations (also in the Boulder vicinity) would be biased toward apparent accuracy by the grid-3 domain being over the Boulder area. This drawback can be addressed with additional studies by 1) running independent studies of the same domain size but different grid spacing and 2) using more case studies.

The improvement in accuracy with decreasing grid spacing is in apparent contradiction with the results of Colle et al. (2000). For precipitation thresholds of less than 5.08 cm day^{-1}, they found that improved resolution did not improve precipitation forecast accuracy (above this threshold, increased resolution improved precipitation accuracy). Because of the lack of comprehensive precipitation observations during this snowstorm, we are unable to say conclusively whether this storm exceeded this threshold. On the basis of the Marshall observations (Fig. 11) and plains-sites observations from Table 1, it did not. We believe the apparent contradiction can then be explained by one of the following: 1) we present a single case study, whereas Colle et al. present a far more comprehensive statistical description; 2) each study used a different mesoscale model; 3) our study is in a polar continental climate, whereas the Colle et al. study represents a maritime polar climate (Whiteman 2000, chapter 6); and 4) the relative importance of orographic detail on mesoscale precipitation variability may be different in this case study as compared with the storms studied by Colle et al. (2000). In addition, for the continental climate of Colorado, a lower precipitation threshold may delineate the point at which higher resolution improves forecast precipitation accuracy. It is clear that more studies are needed to create statistically significant documentation of this capability and thereby to give operational forecasters sufficient confidence in the method.

6. Snowfall evolution: Model versus observations

One of the often-perplexing questions that arises with such accurate model results is, Was the model right for the wrong reasons? That question cannot be answered with absolute certainty here, but we provide some indirect evidence that the model replicates the physics of the precipitation mechanisms during the blizzard and, therefore, may hold promise for accurate snowfall prediction in a variety of cases. The evidence presented below is indirect because it presumes that a relatively accurate forecast of the start and end of precipitation, precipitation rates, and the accumulation of precipitation during the blizzard is a reliable indicator of the quality of model physics. Direct evidence would require, in addition, a comparison of predicted versus observed hydrometeor number density, spectra, and type.

During the blizzard, an intercomparison of various snowfall measurement systems was being completed by the National Center for Atmospheric Research for the National Weather Service in Marshall [see Fig. 9a for location; Wade et al. (1998)]. In the comparison were five different measurement systems that recorded precipitation liquid equivalent throughout the blizzard. In addition, manual snowpan measurements were made for the first 20 h of the ~44 h period of precipitation at Marshall (before the personnel were forced to leave the site because of worsening conditions). The measurements from the five instruments being tested and the manual data are shown in Fig. 11. One item to note is that the scatter among the final precipitation totals of the various systems is large; the lowest is 26 mm [ETI, Inc., all-weather precipitation accumulation gauge (AWPAG)] and the highest is more than 63 mm [not shown; see Wade et al. (1998)]. To choose a measurement for comparison with the model output, we consulted with C. Wade of NCAR (1999, personal communication), who informed us that, based on experience and primarily the coincident, carefully executed, snowpan measurements, the 15-min-interval ETI (Wyoming shield) measurement is considered the most accurate representation of the blizzard precipitation evolution. This conclusion is further verified in Wade et al. (1998).

To create an unprecedented comparison of modeled snowfall (precipitation) rates with accurate, high-frequency, snowfall measurements, we have plotted the 30-min cumulative precipitation predicted by RAMS at Marshall for the three different simulations versus the 15-min-interval observations. Using the ETI Wyoming shield precipitation measurement for comparison, the Bliz48S2 run predicts total precipitation 4% low, the Bliz60R1 run is 21% low, and the Bliz60S1 run is 4% high. As with the overall statistics on grid 3, the Schultz (1995) microphysics has less total precipitation error than the full RAMS microphysics (assuming the ETI Wyoming measurement is, indeed, the most accurate measurement of actual precipitation). The relative accuracy of the evolution of precipitation is addressed below. We be-

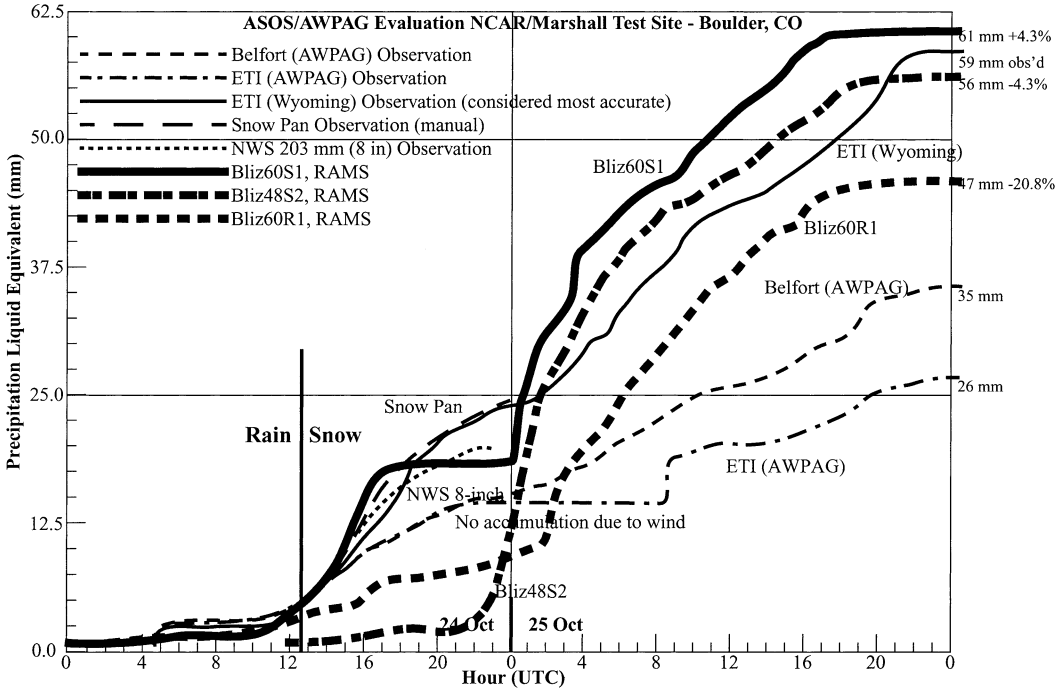

FIG. 11. MAR snowfall measurements systems records compared with the precipitation modeled in three RAMS simulations for the 24–26 Oct 1997 blizzard in the Colorado Front Range: Bliz60S1, Bliz48S2, and Bliz60R1. The ETI-Wyoming measurement is considered to be the most accurate. [Partially adapted from Wade et al. (1998).]

lieve that this is the first high-temporal-resolution comparison of modeled precipitation with measured precipitation, particularly in the case of an extreme-weather event.

We can use the time intervals of the ETI Wyoming gauge, which represent the actual evolution of snowfall at the Marshall site, to verify how well the model physics represented the evolution of storm intensity. If we compare the Bliz60R1 plot in Fig. 11 with the ETI Wyoming evolution, we see that the snowfall has an intensity that is too low from 1200 to 2200 UTC 24 October, resulting in a precipitation total that is less than one-half of the actual total by 0200 UTC 25 October. However, the modeled precipitation does continue to increase during the period 1700–0200 UTC, whereas the precipitation in Bliz60S1 does not. At 0200 UTC, the precipitation rate in this simulation increases drastically (~6 mm in 30 min); it is unclear what causes this behavior (or whether it is inaccurate, because precipitation rates of this magnitude, combined with blizzard winds, can test the performance characteristics of any precipitation measurement system). After that time the precipitation rate is consistent with that measured through 1700 UTC 25 October, after which the precipitation ends. The modeled end of precipitation at Marshall is about 5 h earlier than recorded. So, although the total accumulation of precipitation by Bliz60R1 is somewhat low, the overall evolution has a number of favorable aspects.

Comparison of the Bliz60S1 results with the ETI (Wyoming) measurements in Fig. 11 shows higher correlation than for Bliz60R1. Precipitation begins at a slow rate from 0400 to 1200 UTC 24 October, nearly matching the low total amount of precipitation measured by the ETI Wyoming at the end of that period. From 1200 to 1700 UTC, the actual precipitation rate increases significantly, and this simulation slightly overpredicts that precipitation rate. At 1700 UTC, the modeled precipitation is about 2.5 mm too high. After 1700 UTC 24 October through 0000 UTC 25 October, the modeled precipitation deviates significantly from the continued accumulation of actual precipitation, with no accumulation of model precipitation. An evaluation of the forecast Eta fields that were used for nudging during this period of limited precipitation indicates that the reduced precipitation rates may correspond to a lack of inflow moisture in those fields. Another possible explanation, based on the fact that Bliz60R1 continues to accumulate precipitation during this same period, is that the microphysical process responsible for the precipitation during this time was eliminated by the Schultz (1995) microphysics modification. After 0000 UTC 25 October, the modeled precipitation rate increases dramatically and perhaps unrealistically, allowing the total modeled precipitation again to surpass the measured precipitation. Within two model hours, the precipitation rate decreases to nearly that of the measured precipitation until 1800 UTC 25 October. The modeled precipitation ends 3 h earlier than the measured precipitation with a total of 61 mm versus the observed value of 59 mm. In sum-

mary, although the total precipitation in Bliz60S1 is very accurate and at times the evolution of precipitation rate is very good, some questionable microphysical responses may be present.

A plot of the evolution of the Bliz48S2 precipitation at Marshall is included in Fig. 11 for comparison with the 60-h runs. Although it does not encompass the entire precipitating period, having been initialized at 1200 UTC 24 October, it does mimic an actual forecast that could have been made in real time in 1997 using Eta analyses and boundary conditions. One can see in Fig. 11 that, after a period of model spinup with unrealistic precipitation rates from 2100 UTC 24 October to 0200 UTC 25 October, precipitation rates become more representative after 0200 UTC 25 October, with total precipitation 4% too low when compared with the ETI Wyoming measurement.

7. Summary

This investigation has addressed the heavy snowfall, its distribution, and storm evolution during the 24–25 October 1997 storm in Colorado. The storm not only crippled transportation in the state, producing snowfall amounts that exceeded 1.5 m in less than 48 h, but destroyed about 5300 ha of forest in north-central Colorado. Strong upslope (easterly component) flow forced over very complex orography and embedded within intense large-scale dynamic lift probably controlled much of the snowfall distribution. Investigation of available stability and wind profiles indicated that mechanisms for damaging winds were similar to westerly wind events that have occurred on Colorado's Front Range, which is discussed in detail in Part II using the same RAMS simulations herein. NCEP guidance, though poorly resolved for this storm in complex terrain, was very accurate in its representation of the dynamic structure, including precipitation amounts on the spatial scale for which it was intended.

Three RAMS model simulations of this event are presented with the explicit purpose of showing model capability in reproducing small-scale (meso γ) snowfall variability and storm snowfall (liquid equivalent) evolution. NCEP guidance is used for initialization and subsequent nudging of outermost boundary conditions. Using model resolution (grid spacing) that is high (small) by the standards of NWP, precipitation patterns and amounts are reproduced with reasonable skill. With 5.00-km horizontal grid spacing it is shown that, when using the Schultz (1995) simplified one-moment microphysical scheme, the mean absolute total precipitation error is 41% as compared with observations (those observations are subject to an error themselves, which was not quantifiable here) and that the RAMS full microphysics (Walko et al. 1995) scheme MAPE was 128%. A further reduction in horizontal grid spacing to 1.67 km over the Colorado Front Range portion of the blizzard area resulted in a corresponding improvement in MAPE to 9% and 11%, respectively (see Table 1). These results appear to contradict those of Colle et al. (2000) who found that improved resolution does not improve forecast precipitation accuracy for lower precipitation thresholds, although a number of caveats are described in section 5 for this individual case.

A further comparison was made of modeled snowfall rates with in situ storm measurements. This comparison showed that the model results using two microphysical schemes for snowfall beginning, end, and rate were similar to the natural values during the blizzard, with some exceptions. Each scheme at different times showed favorable behavior, with storm total precipitation eventually favoring the Schultz (1995) scheme. Although this clearly is indirect evidence of the quality of model physics, it implies that the cloud microphysical schemes, in concert with orographic, synoptic, and mesoscale forcing, are representing actual precipitation processes with some degree of accuracy. More detailed and statistically significant investigations are required to clarify this implication.

The ability of the mesoscale model to capture the total snowfall, its meso-γ-scale distribution, and the snowfall rate evolution, as shown herein, demonstrates the potential for improved numerical guidance with higher resolution and more sophisticated physical representation of cloud and precipitation processes. We believe that considerably more research into the capability of mesoscale models run at very high resolutions is justified by the examples discussed herein. Only by doing so will the scientific community be able to determine whether such techniques can consistently deliver similar results, with significant benefits to the public. Although simulations such as these could be completed by a large computer cluster in an operational environment today, the current rate of improvement in computer processing speed means that simulations such as these will be economically and technically achievable by 2005.

Acknowledgments. The authors acknowledge those observers (both official and unofficial) who kindly provided their observations. NOAA/FSL provided the Eta analyses and forecast data. Snowfall amounts were in part supplied by NWS observers, cooperative observers, and Matt Kelsch and Ed Szoke of NOAA/FSL. GSP acknowledges the support of the National Science Foundation, Grants ATM-9713073 and ATM-9816160. Chuck Wade, of the National Center for Atmospheric Research, Research Application Program, Applied Science Group, is acknowledged for kindly providing the Marshall test site precipitation data for the October 1997 blizzard.

REFERENCES

Colle, B. A., and C. F. Mass, 2000: The 5–9 February 1996 flooding event over the Pacific Northwest: Sensitivity studies and eval-

uation of the MM5 precipitation forecasts. *Mon. Wea. Rev.,* **128,** 593–617.

——, K. J. Westrick, and C. F. Mass, 1999: Evaluation of MM5 and Eta-10 precipitation forecasts over the Pacific Northwest during the cool season. *Wea. Forecasting,* **14,** 137–154.

——, C. F. Mass, and K. J. Westrick, 2000: MM5 precipitation verification over the Pacific Northwest during the 1997–99 cool seasons. *Wea. Forecasting,* **15,** 730–744.

——, ——, and D. Ovens, 2001: Evaluation of the timing and strength of MM5 and Eta surface trough passages over the eastern Pacific. *Wea. Forecasting,* **16,** 553–572.

Cotton, W. R., and R. A. Anthes, 1989: *Storm and Cloud Dynamics.* 1st ed. Academic Press, 883 pp.

Doesken, N. J., and A. Judson, 1997: *The Snow Booklet: A Guide to the Science, Climatology, and Measurement of Snow in the United States.* 2d ed. Colorado State University Press, 87 pp.

Dudhia, J., 1993: A nonhydrostatic version of the Penn State–NCAR Mesoscale Model: Validation tests and simulation of an Atlantic cyclone and cold front. *Mon. Wea. Rev.,* **121,** 1493–1513.

Gaudet, B., and W. R. Cotton, 1998: Statistical characteristics of a real-time precipitation forecasting model. *Wea. Forecasting,* **13,** 966–982.

Hodur, R. M., 1997: The Naval Research Laboratory's Coupled Ocean/Atmosphere Mesoscale Prediction System (COAMPS). *Mon. Wea. Rev.,* **125,** 1414–1430.

Junker, N. W., J. Joke, and R. Grumm, 1989: Performance of NMC's regional models. *Wea. Forecasting,* **4,** 368–390.

Marwitz, H., and J. Toth, 1993: The Front Range blizzard of 1990: Part I: Synoptic and mesoscale structure. *Mon. Wea. Rev.,* **121,** 402–415.

Mass, C. F., D. Ovens, K. Westrick, and B. A. Colle, 2002: Does increasing horizontal resolution produce better forecasts? The results of two years of real-time numerical weather prediction over the Pacific Northwest. *Bull. Amer. Meteor. Soc.,* **83,** 407–430.

Pielke, R. A., and Coauthors, 1992: A comprehensive meteorological modeling system—RAMS. *Meteor. Atmos. Phys.,* **49,** 69–91.

Rogers, E., T. Black, B. Ferrier, Y. Lin, D. Parrish, and G. DiMego, cited 2001: Changes to the NCEP Meso Eta Analysis and Forecast System: Increase in resolution, new cloud microphysics, modified precipitation assimilation, modified 3DVAR analysis. [Available online at http://www.emc.ncep.noaa.gov/mmb/mmbpll/eta12tpb.]

Schultz, P., 1995: An explicit cloud physics parameterization for operational numerical weather prediction. *Mon. Wea. Rev.,* **123,** 3331–3343.

Snook, J. S., J. M. Cram, and J. M. Schmidt, 1995: LAPS/RAMS: A nonhydrostatic modeling system configured for operational use. *Tellus,* **47A,** 864–875.

Szoke, E., 1989: Mesoscale structure of winter snowstorms in northeast Colorado as revealed by Doppler radar: Potential for short range forecasting. Preprints, *12th Conf. on Weather Analysis and Forecasting,* Denver, CO, Amer. Meteor. Soc., 384–389.

Wade, C., R. Rasmussen, and J. Cole, 1998: An evaluation of the NWS ASOS candidate all-weather precipitation accumulation gauges (AWPAG) and the LEDWI and the enhanced LEDWI at the NCAR test site at Marshall, Colorado, February–November 1997. Final Rep., NCAR, 123 pp. [Available from Applied Science Group, Research Application Program, National Center for Atmospheric Research, Boulder, CO 80303.]

Walko, R. L., W. R. Cotton, M. P. Meyers, and J. L. Harrington, 1995: New RAMS cloud microphysics parameterization. Part I: The single-moment scheme. *Atmos. Res.,* **38,** 29–62.

Wesley, D. A., J. Weaver, and R. Pielke, 1990: Heavy snowfall during an arctic outbreak along the Colorado Front Range. *Natl. Wea. Dig.,* **15,** 2–19.

——, B. Bernstein, and R. Rasmussen, 1995: Snowfall associated with a terrain-induced convergence zone during the Winter Icing and Storms Project. *Mon. Wea. Rev.,* **123,** 2957–2977.

Whiteman, C. D., 2000: *Mountain Meteorology: Fundamentals and Applications.* 1st ed. Oxford University Press, 355 pp.